

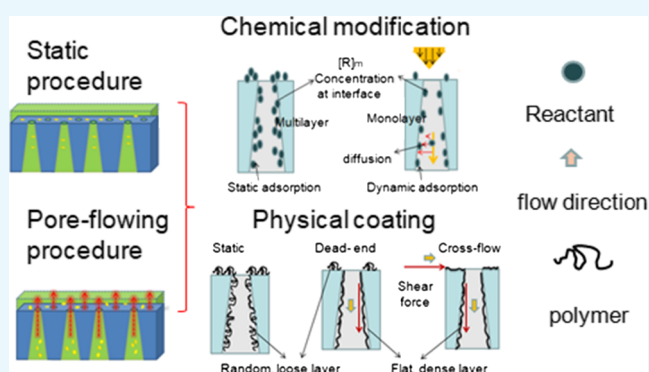
Surface Modification of Polyacrylonitrile Membrane by Chemical Reaction and Physical Coating: Comparison between Static and Pore-Flowing Procedures

Yang Qin, Hu Yang,*^{ORCID} Zhenliang Xu,^{ORCID} and Feng Li

Membrane Research Center, Chemical Engineering Research Institute, East China University of Science and Technology, Shanghai 200237, PR China

S Supporting Information

ABSTRACT: The influences of static and pore-flowing procedures on the surface modification of a polyacrylonitrile (PAN) ultrafiltration membrane through chemical reaction and physical coating were investigated in detail. For chemical modification by ethanolamine, a membrane modified by the pore-flowing procedure showed a higher flux and different morphology. The reasons were explained by two effects: the pore-flowing resistance to the random thermal motion of PAN at high temperatures and different reaction kinetics related to the reactant concentration profile on the interface between the membrane and reaction solution and the kinetic property of the fluid (driving force and miscibility) and reaction (time and rate). For physical coating modification, a dense and flat layer via a loose and random layer was formed during the pore-flowing process and static process, which changed the flux and antifouling property of the membrane. The membrane prepared by dead-end filtration showed the best trade-off between the flux and antifouling property. Overall, the procedure kinetics plays an important role in the optimization of membrane modification.



1. INTRODUCTION

Membrane fouling during a pressure-driven membrane separation process could seriously decline both the permeability and selectivity of the membrane and shorten its lifespan.^{1,2} Among the different fouling components, organic fouling has done the greatest damage, which was mainly caused by the irreversible adsorption of organic matter. The research showed that the hydrophilic surface could effectively reduce such irreversible adsorption.³ Surface modifications, including physical coating and chemical modification,^{4,5} were widely used to prepare hydrophilic membrane.

The main advantages of surface modifications lie in their simple and flexible procedure without changing the property of the membrane matrix. For example, different modification technologies, such as physical and chemical modifications, can be integrated to improve their effect.^{8–10} Although the hydrophilic membrane can also be prepared by using amphiphilic copolymers directly during the membrane preparation process, the multistep synthesis procedure and expensive price weaken their attraction.^{6,7}

During the surface modification process, the optimization of the morphology and chemical composition of the modified layer is the key to improve the property of the membrane.^{11–13} Usually, the difference in the molecular shape of the reactant, the number of functional groups, or the modification method can produce layers of different topologies.^{14–16} Moreover, the

reaction direction, such as grafting-from and grafting-to, can produce modified layers with different grafting densities, chain lengths, coverages, and thicknesses.^{17–19} Besides, a regular modified layer is also the basic requirement for further functionalization of the membrane.^{20,21}

Up to now, many efforts have been devoted to update the membrane modification with new technologies, such as atom transfer radical polymerization, fixation of initiator, click chemistry, and so forth.^{22–24} However, one aspect of the modification that is the process kinetics has been long ignored. From the point of view of chemical engineering, the mass transfer and diffusion of reactants play an important role in the chemical process.^{25–27} Virtually, their influence has been reflected in the membrane preparation process, only their importance is ignored. For example, Sejoubari et al. proposed a “grafting-through” method, in which monomers were supplied through the surface by diffusion.²⁸ Also, grafting with the monomer vapor was different compared with grafting in the solution.²⁹ The interface reaction has been widely used to synthesize the nanofiltration membrane.^{30–33} The diffusion of reactant during the interface reaction can significantly influence the property of the membrane.

Received: December 31, 2017

Accepted: April 2, 2018

Published: April 16, 2018

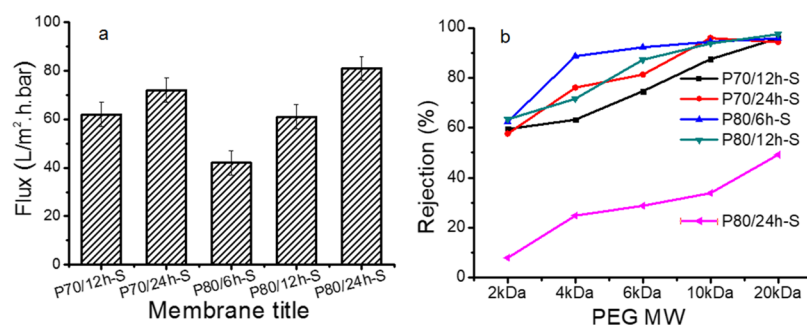


Figure 1. Influence of modification time on the flux (a) and rejection (b) of ETA-modified PAN membranes by the static method, using 6% ETA aqueous solution.

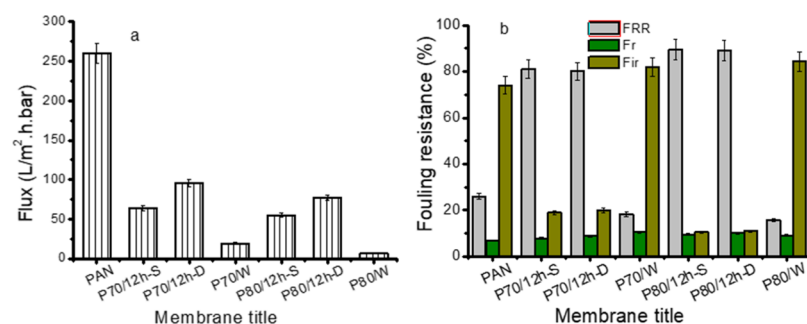


Figure 2. Pure water flux (a) and antifouling properties (b) of PAN membranes modified by different procedures.

During the surface chemical modification, the reaction rate depends on the reactant concentration at the interface and the reaction region is related to the distribution of reactant. Similarly, physical coating by the polymer, which is a typical surface adsorption process, can be influenced by the morphology profile of the polymer on the interface. All of these will be interfered by the flow state of reactant or polymer in the modification process. That is, the kinetic property of the modification process could play an important role in tailoring the property of the modified membrane. To the best of our knowledge, no such research has been carried out up to now.

A polyacrylonitrile (PAN) membrane is cheap and popular for various applications.^{34–37} Similarly, surface modification is also frequently used to improve the property of PAN membrane.^{38,39} Multistep chemical modifications based on hydrolysis reaction and nucleophilic addition are also frequently reported.^{40–42} The coating method is also applied for PAN modification, including polymer, nanoparticles, and so forth.^{43–45}

In the present study, both chemical modification and physical coating were investigated as the representative modification processes for all types of membranes.^{42,44} A simple, chemical ethanolamine (ETA) was chosen to react with nitrile groups of PAN,^{46,47} which can be replaced by other functional amines in principle. The static and pore-flowing procedures were applied to compare their modification difference. It is interesting to find that the process kinetics, such as flowing, reaction, and adsorption, could influence the morphology and the performance of the modified membrane. The results provide new knowledge for the membrane modification process.

2. RESULTS AND DISCUSSION

2.1. Modification by ETA. 2.1.1. Static Modification.

First, the modification temperature was optimized. The modification was very slow at the temperature lower than 70

°C (shown in Supporting Information Figures S1 and S2). Therefore, the modification temperature was set between 70 and 80 °C. The influence of time was investigated. The results are shown in Figure 1.

The ETA-modified membrane had a lower water flux than that of the pristine PAN membrane. In general, high-temperature treatment should be beneficial to the radial shrinkage of the membrane matrix, which will result in a decrease in the pore size and a decrease in the flux.⁴⁸ Essentially, such phenomenon is related to the intensified thermal motion of the polymer. In Figure 1, the flux of the modified membrane increased with the reaction time, which means that the modification is favorable to improve the flux. The reason should be due to the improved hydrophilicity after modification. The improved hydrophilicity enables more water molecules to be adsorbed by the polymer which facilitate the diffusion of water through the PAN membrane. This is quite popular for the hydrophilic modification process. Moreover, the adsorbed water may also retard the thermal motion of PAN somehow. Therefore, these factors caused increased flux of the membrane after modification.

The rejection was shown in Figure 1b. After modification, the molecular weight cutoff (MWCO) of the PAN membrane decreased, which means the modified PAN membranes have a better selectivity. Within all five membranes, P80/12h-S has a better comprehensive separation property. Although P80/24h-S has a higher flux due to the higher modification degree, it shows a lower selectivity. Moreover, the mechanical property was also measured (shown in Supporting Information Table S1). Modification improved the mechanical property of the membrane. However, 24 h modification caused a slight decrease in the tensile strength compared with that of 12 h modification. This could be attributed to a looser packing between original PAN molecules after a higher modification.

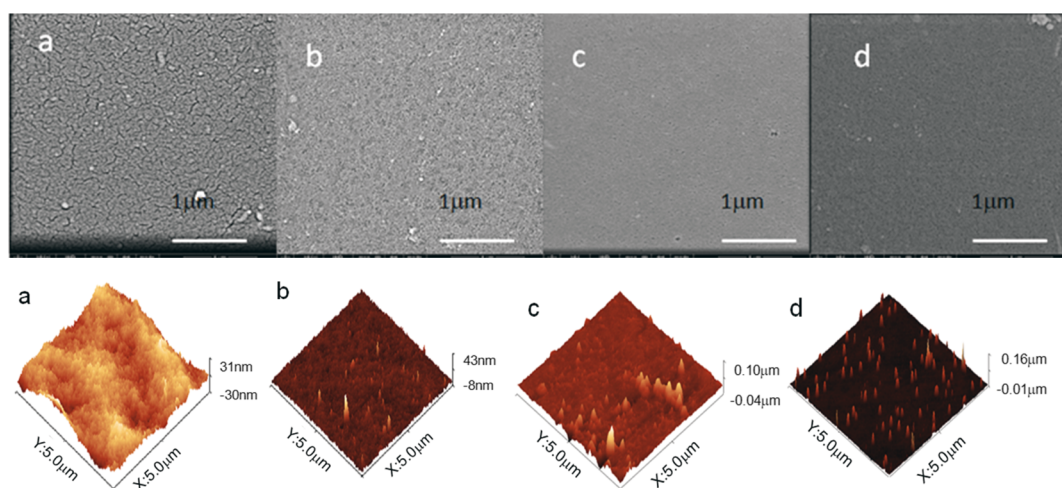


Figure 3. SEM and AFM images of PAN membranes modified at different conditions: (a) PAN, (b) P70/W, (c) P70/12h-S, and (d) P70/12h-D.

2.1.2. Comparison between Static Modification and Pore-Flowing Modification (Self-Weight Driving). **2.1.2.1. Longer Time Modification.** According to the results in the static procedure, 70–80 °C and 12 h were chosen as the optimized conditions. The separation performance of the modified membranes is shown in Figure 2.

In Figure 2a, membranes P70/W and P80/W (modified by pure water) showed a very low flux, whereas the modified membrane has a higher flux. As explained above, the intensified thermal motion of the polymer may narrow the pore window of the membrane. Such effect becomes much obvious at higher temperatures. The increased water flux of the ETA-modified membrane should be attributed to the improved hydrophilic property after modification. Both membranes P80/12h-D and P70/12h-D showed higher flux than that of membranes P80/12h-S and P70/12h-S, whereas their difference in selectivity is not very much. That is, PEG20k rejection is 91% for P70/12h-D and 95% for P70/12h-S. For the membrane modified at 80 °C, the flux difference caused by two procedures is less than that modified at 70 °C. This could be related to the intensified thermal motion of PAN chains.

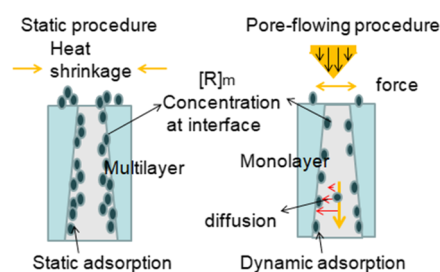
The increased flux for the pore-flowing procedure can be explained by several reasons. First, the solution flow enhanced its resistance to the random thermal motion of PAN chains in the pore-flowing procedure, whereas in the static procedure, PAN chains were in a free state to respond to the thermal strain. Second, the reaction kinetics was changed by the flow process, which is related to the reactant concentration, $[R]_m$, at the interface between the membrane and ETA solution. This will be explained in detail later. Finally, because the membrane was fixed by the equipment during the pore-flowing procedure, it may influence the free movement of PAN chains in the membrane more or less, although no measurable volume change was observed during the modification process.

The antifouling properties are shown in Figure 2b. The flux recovery ratio (FRR) data of the modified membrane increased with the temperature were about 80% (modified at 70 °C) and 90% (modified at 80 °C), much larger than that of the pristine PAN membrane. This was due to the improved hydrophilic property or modification degree. Moreover, P80/12h-D and P80/12h-S and P70/12h-D and P70/12h-S showed the similar FRR and flux irreversible (Fir) data. Therefore, it means that the pore-flowing procedure is suitable to prepare the membrane

with higher flux and lower selectivity. The static procedure is just the opposite.

The surface scanning electron microscopy (SEM) and atomic force microscopy (AFM) images of PAN membranes modified at 70 °C were measured and are shown in Figure 3. The pristine PAN membrane showed a fissure structure on its surface. Such fissures began to disappear after heat water treatment, which proved the shrinkage effect caused by the intensified thermal motion of PAN chains at high temperatures. Although the modified PAN membranes showed a similar smooth surface in SEM, AFM images provided a clear difference for two membranes in detail: a random homogeneous surface for P70/12h-S and a rough but evenly distributed modification on certain areas for P70/12h-D. Such variation could be explained by the pore-flowing effect and the different reaction kinetics features of two procedures, as shown in Scheme 1.

Scheme 1. Illustration of the Difference in Chemical Modification during Static and Pore-Flowing Procedures



First, the pore-flowing effect restrains the movement of thermal motion of PAN chains, so they are unable to move freely to release the thermal strain caused by high temperature as in the static procedure. This is also the reason for different AFM roughnesses of the membrane. Second, the reaction process is also different for two procedures because the reaction rate is related to the concentration of the reactant at the interface $[R]_m$, in Scheme 1. For static process, $[R]_m$ obeyed the physical adsorption principle, which showed the character of multilayer, whereas for the pore-flowing procedure, the reactant adsorption was interfered by the shear force caused by the flow. The ETA molecules weakly adsorbed on the interface could be easily washed away by the flow. Therefore, a

monolayer adsorption was formed. That is, the reaction is in disadvantage during the pore-flowing process. Moreover, the diffusion of reactant from the center of the solution to the interface was also different for two procedures, which could also influence the reaction process.

Energy-dispersive spectrometer (EDS) data (mapping scan) of the modified membranes are shown in Table 1. Because

Table 1. EDS Data of PAN Membranes Modified by Different Methods

element	PAN (atom %)	P70/12h-D (atom %)	P70/12h-S (atom %)
C K	84.02	71.26	69.7
N K	13.35	20.24	21.52
O K	2.62	8.5	8.78

chemical modification only formed a single monolayer, the atom content on the surface virtually reflected the modification degree. In Table 1, P70/12h-S showed a higher N, O content than that of P70/12h-D. This proved our above analysis that the flowing process was unfavorable for the reaction. It showed stronger selectivity for the reaction area.

2.1.2.2. Shorter Time Modification. To weaken the influence of temperature, the modification process was further carried out for a shorter time by increasing the ETA concentration. The results are shown in Figure 4.

The flux change of the modified membrane is the trade-off between the modification degree and heat effect. In Figure 4a, for each group, the membrane modified by the pore-flowing procedure showed a higher flux than that modified by the static procedure in spite of different modification conditions. For antifouling property shown in Figure 4b, FRR increased from 40% (membranes: P70/E50-1h-S/D) to 85% (membrane: P70/E12-6h-S/D), in Figure 7b. Unlike flux, the FRR data are very sensitive to the hydrophilicity of the membrane or the modification degree. Thus, it can be thought as the reflection of the modification degree. In other words, two membranes have the similar modification degree in each group. Therefore, the results reprove the conclusion that the pore-flowing procedure tended to produce membrane with larger flux when the membrane was modified to the similar extent.

As for P30/E30-3h-D/S, it showed a lower antifouling property and lower flux compared with those of P70/E12-6h-D/S, which is due to its lower modification degree (FRR data). On the other side, its FRR was similar to that of P70/E50-1h-D/S, but it took longer reaction time, so its flux is lower than the latter.

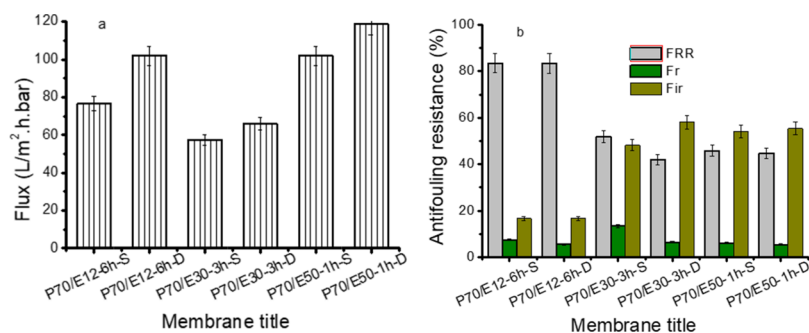


Figure 4. Water fluxes (a) and antifouling properties (b) of PAN membranes modified at 70 °C by increasing the ETA concentration and decreasing the time.

AFM images are shown in Figure 5. The membrane modified by the static procedure through different reaction conditions

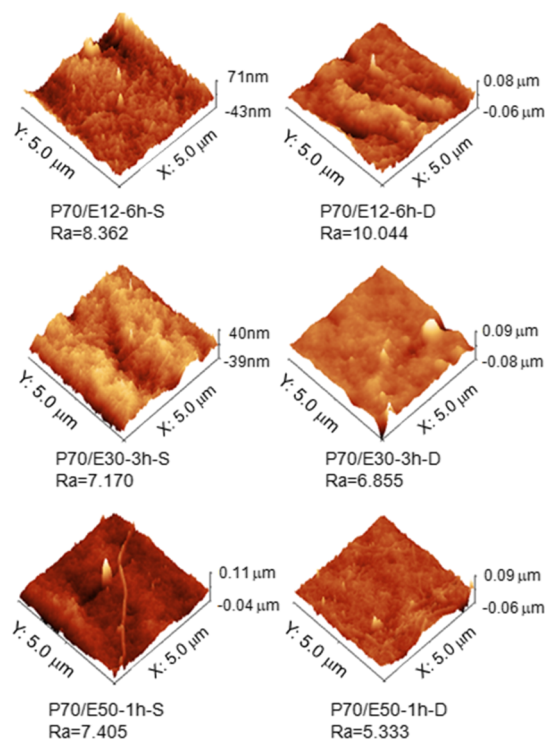


Figure 5. AFM images of PAN membranes modified at different reaction times and ETA concentrations through static and pore-flowing procedures (driving by self-weight).

showed the similar surface roughness, whereas the surface roughness increased with the modification degree (FRR data) for membranes modified by the pore-flowing procedure. As explained above, the membrane was in a free state during the static process. Therefore, the morphology has less relationship with the modification degree. For the pore-flowing procedure, the pore deformation of the membrane was resisted by the flow of the liquid. Such effect became much obvious with the prolonged treating time. Moreover, the surface reaction degree was not all the same for the whole surface area in the pore-flowing process. That is why the surface morphology difference of the modified membrane was enlarged with the increased modification degree.

Although it is difficult to evaluate the individual contribution of time or concentration to the modification degree because the

Table 2. Properties of Some Modified PAN and Other Antifouling Ultrafiltration Membranes in the Literature

modification method or membrane material	flux (L/m ² ·h·bar) and FRR (BSA)	rejection	FRR change (PAN) ^a	flux ratio (PAN) ^a	refs
coating [polyethyleneimine (PEI) + Cu ²⁺]	PAN-PEI-Cu, flux: 63 (at 0.16 MPa)	HA: 91%		63/128	49
hydrolysis ^a /poly(AN-co-meth acrylic acid) membrane	flux: 28–150 at 1.5 kg/cm ²	MWCO: 9–75 kDa	from 53 to 91%	(28–150)/215	50
hydrolysis + reaction (with DETA ^d + PFOA ^e)	PAN-PFOA, flux: 89	BSA: 99.5%	from 58 to 96% ^c	90/150	37
hydrolysis + reaction (with PEG)	PAN-PEG, flux: 40		from 64 to 77%	40/56	40
hydrolysis + reaction (with oligodeoxynucleotide)	modified PAN, flux: 79	BSA: 93%	from 41 to 89%	77/79	51
hydrolysis + reaction (with PEI-based zwitterion)	Z(PEI)-PAN, flux: 125	BSA: 99%	from 78 to 99.8% ^c	140/160	52
hydrolysis + coating (tetraethyl orthosilicate)	PAN-SiO ₂ , flux: 58	PEG6000: 90%	from 76 to 91%	58/605	53
additive ^f (PAN-g-poly(vinyl alcohol))/PAN (hollow fiber)	flux: 140	trypsin: 74%	from 75 to 85%	140/41	54
coating (sulfonated poly-aniline)/PVDF membrane	PVDF/SPANI, flux: 160	BSA: 90%	from 65 to 95% ^g		55
additive (PU)/PVDF membrane	PU-PVDF (adding 4%), flux: 181	BSA: 90%	90%		56
reaction (with ETA)/PAN membrane	P70/E12-6h-D, flux: 100	PEG20000: 91%	from 28 to 82%	100/260	this study

^aCompared with the nascent PAN membrane. ^bHydrolysis: NaOH treatment. ^cBSA solution with buffer. ^dEDTA: diethylenetriamine. ^ePFOA: pentadecafluorooctanoic acid. ^fMembrane prepared by the NIPS method using special additive, shown in brace. ^gMembrane was taken out and immersed in the phosphate butter for 10 min and rinsed with pure water for 20 min.

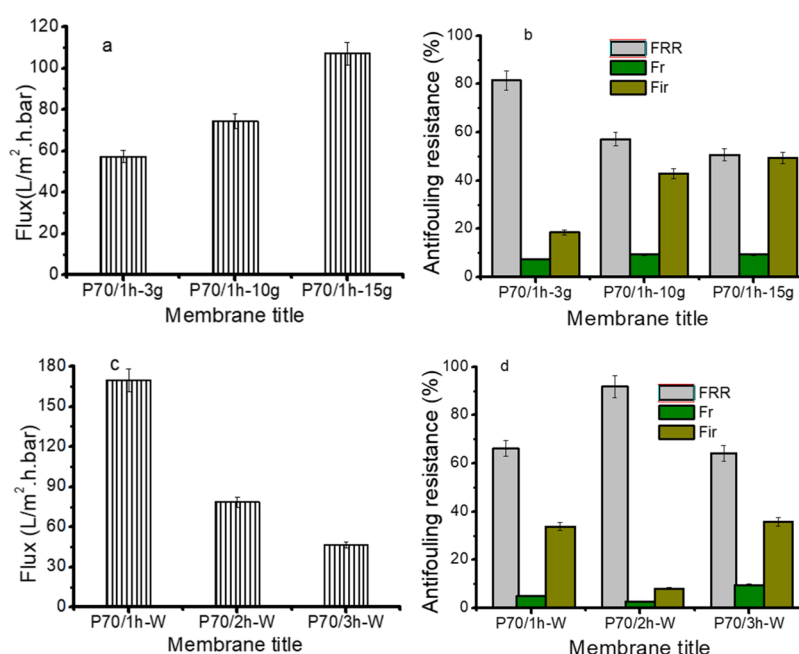


Figure 6. Water fluxes and antifouling properties of the modified PAN membranes by the pore-flowing procedure, driven by N₂ gas (a,b) and by vacuum (c,d).

above three groups were modified at different conditions (ETA concentration and time), we can still make a rough estimate on their difference. According to reaction kinetics, the modification degree is related to the reaction rate and reaction time. The reaction rate is in proportion to the reactant concentration, $[R]_m$, because $[R]_m$ is normally much higher than that in the solution due to the physical adsorption principle. Therefore, the increased $[R]_m$ data caused by increasing the solution concentration was not so large. That is why the membrane modified at 50% ETA but for a short time still has a low FRR data. This is also in agreement with our former conclusion. ETA modification is a slow reaction; it needs higher temperature or longer time.

Finally, the performance of our modified membranes was compared with those reports in the literature to give a comprehensive evaluation, although our main intention is to find an optimized routine. The results are shown in Table 2.

It can be found that our membranes show a competitive performance. There are some very high FRR data in Table 2, which should be attributed to different experimental conditions because the antifouling property of the membrane can be influenced by the pH value and ion strength of the solution. That is, their nascent PAN membrane showed a FRR about 77% for the BSA solution filtration,⁵² whereas our fresh PAN membrane showed only about 28% FRR.

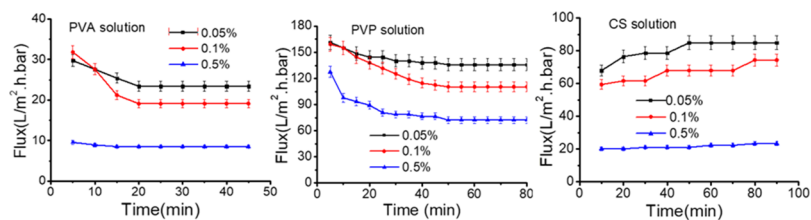


Figure 7. Water flux decay of the PAN membrane during the filtration of PVA, PVP, and CS solutions with different concentrations (0.5, 0.1, and 0.05%, respectively).

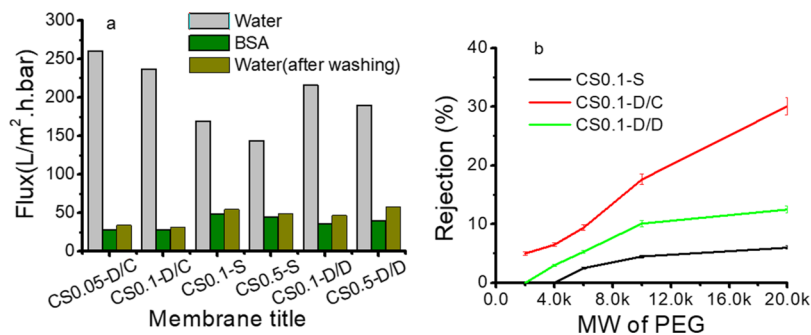


Figure 8. Water flux, antifouling property (a) and rejection (b) of the modified PAN membrane by CS solution (CSN-D/S/C,D: N: concentration of CS, D/S: pore-flowing modification/static treatment, and C,D: cross-flow, dead-end filtration).

2.1.3. Pore-Flowing Modification by Different Driving Forces. Because the driven forces could influence both the flowing kinetics and the reaction kinetics, gas pressure and vacuum were used to replace the self-weight driving force. Pure ETA was used to shorten the modification time and reduce the shrinkage effect. The results are shown in Figure 6.

In Figure 6a,b, N₂ gas pressure was used as a driving force, which was generated due to the decomposition of azobisisobutyronitrile (AIBN).⁵⁷ It could flow through the pore channels of the PAN membrane wetted with ETA and changed the modification process. The water flux of the modified membrane increased with the amount of AIBN, which was in proportion to the pressure of N₂, whereas FRR decreased with the gas amount. High flux and low FRR means a low modification degree. The result showed that the flowing rate (in proportion to pressure) of the media can significantly influence the modification efficiency.

In Figure 6c,d, water vapor was driven by vacuum through the pore channel because ETA has a melting temperature of 170 °C. Compared P70/1h-W with P70/1h-15g, which were prepared under the similar condition except the flow media, P70/1h-W showed much better performance than P70/1h-15g. The reason could be related to the different flowing rate and better miscibility between ETA and water. This result further proved that the physical–chemical property of the fluid was also important. Moreover, P70/2h-W showed the best FRR data. This should be attributed to the property change of the fluid. After a long reaction time, many ETA molecules were also taken away by vacuum. With the changing fluid composition, the surface property of the modified membrane was influenced and its antifouling property was weakened.

In all, the above discussion reveals that the flowing kinetics and the physical–chemical property of the fluid have a great influence on the chemical modification process. Although those conclusion were mainly drawn from the reaction at high temperatures, which was interfered by the heat motion of PAN

chains, it could be still helpful for the modification process at room temperature.

2.2. Physical Coating by Static and Pore-Flowing Procedures.

2.2.1. Selection of Polymer. Physical coating was carried out at room temperature to avoid the interference by temperature. First, the potentials of three polymers, polyvinyl alcohol (PVA), polyvinyl pyrrolidone (PVP), and chitosan (CS), to form a coating layer were evaluated because they all showed a good antifouling property.^{58,59} The water flux curves of PAN membranes during the filtration of the low-concentration solutions via time are shown in Figure 7.

In Figure 7, the membrane flux decreased quickly during the filtration of polymer solution. Less than 40 min, the flux becomes stable for PVA and PVP. A slightly increased flux after 40 min during the filtration of 0.05 and 0.1% CS solution was caused by the slow degradation of CS in a freshly made acidic solution at the beginning. The decreased flux was mainly caused by the physical adsorption of polymer on the membrane surface, similar to the protein filtration process. Because a low-concentration solution was tested, the interaction between polymer chains in the solution can be ignored. When the balance between adsorption and desorption was reached, the membrane flux became steady. Here, the PVA solution significantly decreased the membrane flux. The PVP solution had the smallest influence on the membrane flux. However, its postcross-linking step required a high temperature.⁶⁰ The CS solution showed a moderate influence, so it was chosen for PAN membrane modification.

2.2.2. Comparison of Different Physical Coating Procedures. After dipping the CS-coated PAN membrane into a NaOH solution, the adsorbed CS layer can be fixed on the surface of the PAN membrane. Here, three types of CS-coated PAN membranes were prepared by different procedures. The change in their performance should be caused by the different features of three procedures. Their filtration data are shown in Figure 8a. An obvious change can be observed for membranes modified by different procedures (static adsorption, dead-end

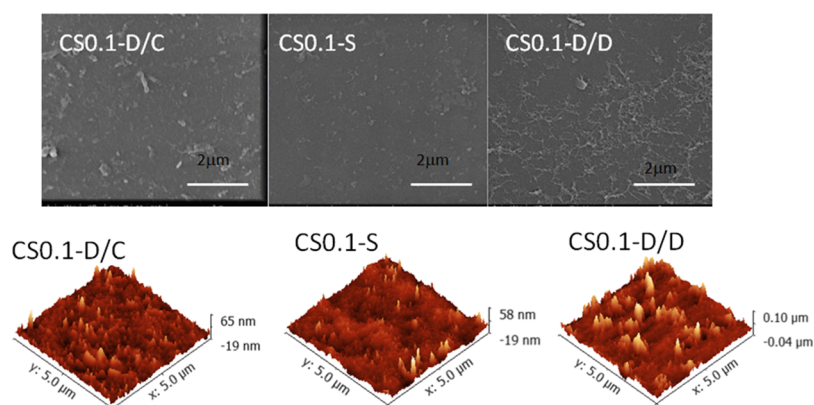


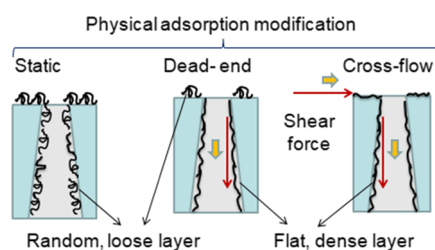
Figure 9. SEM and AFM images of CS-coated PAN membranes by different procedures.

flow, and cross-flow). For three membranes modified with 0.1% CS concentration, CS0.1-D/C (prepared by cross-flowing filtration) had the highest water flux and the lowest water recovery flux. CS0.1-D/D (prepared by dead-end filtration) showed the best balance between the pure water flux and water recovery flux. CS0.1-S (prepared by static adsorption) showed the lowest flux and better water recovery flux. Such difference should be related to the morphology of adsorbed polymer layers on the membrane surface. Compared with the different CS concentrations, membranes modified with a higher CS concentration showed a lower water flux. The reason could be related to the loose CS layer related to the lower concentration of CS. The rejection data of three membranes are shown in Figure 8b; CS0.1-D/C showed the lowest MWCO, which means the smallest pores on the surface. This could be caused by the entrapping effect of the pores on the surface during the cross-flow. To further reveal the reason for such a change, the morphology of the membrane was investigated.

The SEM and AFM images of CS-coated PAN membranes after deposition are shown in Figure 9. Although the deposition of CS on the membrane surface may change its morphology of the adsorbed CS layer, its main features should be still preserved. For the static process, the membrane showed a homogeneously coated surface. For the membrane prepared by dead-end filtration, the surface showed a network-like and rough structure of the CS layer, whereas the membrane prepared by the cross-flowing procedure showed a mediate rough surface.

Such difference in the morphology and membrane performance should be attributed to the influence of the procedure kinetics during the physical coating process. The possible reason is illustrated in Scheme 2, which can be explained according to the different morphology and density of the adsorbed layer.

Scheme 2. Different Coating Layer Morphologies Caused by Different Modification Procedures



For the cross-flowing process, the adsorbed layer was thinner but denser because only those strongly adsorbed polymers could resist the shear force caused by the flow. For static adsorption, a loose and random adsorption structure was formed. Dead-end filtration is like the transition state of two processes. The surface was less influenced than the pore channel by the flow. Such difference changed the morphology and performance on the modified membrane. Moreover, for cross-flowing filtration, the strong shear force on the surface may cause some CS molecules strongly adhering on the pore entrance and decreased the pore size.

Finally, the surface EDS data (mapping scan) are shown in Table 3.

Table 3. EDS Data of the PAN Membrane Coated by 0.1% CS through Different Procedures

element	CS0.1-D/C (atom %)	CS0.1-S (atom %)	CS0.1-D/D (atom %)
C K	70.66	70.65	72.16
N K	24.24	23.61	23.29
O K	5.1	5.74	4.55

In Table 3, CS0.1-S showed a higher N, O ratio than that of CS0.1-D/C. CS0.1-D/D had the lowest N, O ratio. Unlike chemical modification, CS coating formed a multilayer morphology. The surface atom content reflected the dispersion of the CS layer on the membrane surface, not the total adsorption amount of CS on the membrane because those membranes have different surface coverages of CS. The homogeneous coverage of CS should lead to high EDS data, such as CS0.1-S. CS0.1-D/D showed a clear difference between the nonporous area and the entrance of the pore on the membrane surface. Therefore, its average CS content divided by the total surface area was the lowest. Moreover, if the surface morphology and the membrane performance are analyzed together, we can deduce that different areas of the membrane surface (nonporous area or pore entrance) play different roles in improving the antifouling property of the membrane.

3. CONCLUSIONS

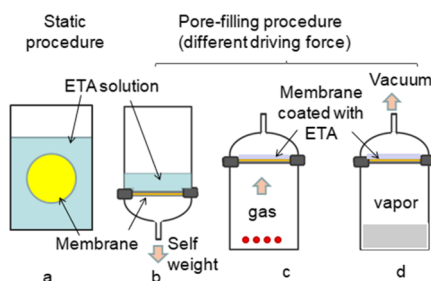
The kinetics of the modification process has a great influence on the properties and structure of the modified PAN membrane. For chemical modification, the membrane was in a free state to correspond to the stress caused by heat and chemical modification during the static procedure. During the pore-flowing procedure, the shrinkage of the membrane can be

ameliorated by the pore flow effect. The reaction process was also influenced by the concentration profile of the reactant on the interface and the kinetic property of the fluid. For physical coating modification, static process was favorable to form a loose and random layer, whereas the pore-flowing procedure was favorable to form a flat but dense layer on the pore channel. In all, the pore-flowing procedure can be used to precisely construct the modified surface and improve the performance of the membrane.

4. EXPERIMENTAL SECTION

4.1. Membrane Preparation. The PAN membrane was prepared by a nonsolvent-induced phase separation (NIPS) method, using 15% PAN dimethyl sulfoxide solution as the casting solution.

Scheme 3. Schematic Illustration of Different Modification Strategies



4.2. ETA Modification. The details of the surface modification of the PAN membrane are shown in Scheme 3 and explained as follows:

- Static modification: the membrane was put into a Ziplock bag filled with ETA solution. The bag was then sealed and put in an oven for modification at different temperatures.
- Pore-flowing procedure (driven by self-weight of the solution): a kettle filled with ETA solution was sealed with a PAN membrane, and then the kettle was placed upside down and put into the oven for modification. The membrane faced up.
- Pore-flowing procedure (driven by gas pressure): a certain amount of AIBN was put into a kettle, and then the kettle was sealed with a PAN membrane and put into an oven for modification. AIBN was used to generate N_2 gas during the reaction.⁵⁷
- Pore-flowing procedure (driven by vacuum plus water vapor pressure): a kettle filled with some waters was sealed with a PAN membrane and put into an oven, and then the kettle was connected with a water pump to get a negative pressure in the kettle.

In processes c and d, the membrane wetted by ETA was used, which was further covered with a polyethylene terephthalate nonwoven wetted with ETA. After modification, the membrane was taken out and washed with water to remove the residual ETA. The preparation conditions and membrane list are shown in Table 4.

4.3. Polymer Coating Modification. The filtration of polymer solution (0.05, 0.1, and 0.5 w/w %) through the PAN membrane was carried out by the pore-flowing procedure. The

Table 4. Experimental Parameters and Corresponding Membranes Obtained by ETA Modification

membrane no.	modify procedure	reactant or solution	flow media	temp (°C)	time (h)
PAN					
P-T/W	a	water	no	T	12
P-T/12h-S	a	6% ETA	no	T	12
P-T/12h-D	b	6% ETA	no	T	12
P-T/E-t	b	ETA (12%, 20%, 50%)	ETA solution	T	t (1, 3, 5)
P-T/t-g	c	ETA	N_2 (g, AIBN)	T	t
P-T/t-W	d	ETA	water vapor	T	t

cross-flowing filtration and dead-end filtration (filtration driven by vacuum) were applied to form a coating layer on the PAN membrane. Then, the coated membrane was taken out for the post-treatment. For the static treatment, the PAN membrane was immersed into a polymer solution for the same time as the filtration process.

For the post-treatment, the CS-coated membranes were immersed into 1% NaOH solution for half an hour. Because CS is insoluble in alkaline solution, it will deposit and form a fixed layer on the surface of the PAN membrane.

4.4. Characterization of the Membrane. Dynamic contact angle was measured by a contact angle analyzer (JC2000D1, Shanghai Zhongchen Digital Technology Apparatus Co. Ltd., China). A water droplet of 0.2 mL was transferred from a needle tip onto the membrane surface. The machine was coupled with a camera, enabling image capture at 10 frames/s. A series of images were captured at a constant time rate to measure the contact angle. SEM was measured by JSM-5600LV (JEOL Co., Japan). The instrument uses an electron beam accelerated at 3 kV. To obtain the cross section, a dry membrane was immersed in liquid nitrogen and fractured and the fractured surface sputtered with a thin layer of gold prior to SEM analysis. EDS mapping scan was measured by QUANTAX 400-30 installed on SEM. The distribution and relative proportion (intensity) of elements over SEM image were mapped. The surface roughness was investigated by AFM (NanoScope IIIa MultiMode, USA) in a scan size of 500×500 nm by the tapping mode. 256 scans were taken per image. The surface roughness parameters were reflected in terms of the average roughness (R_a) and the root-mean-square roughness.

4.5. Membrane Filtration. A self-made cross-flowing cell (an effective area of 28.26 cm^2) was adopted to evaluate the flux (J) and rejection (R) of PAN membranes. The PAN membranes were prepressured at 0.1 MPa with pure water for 0.5 h at $25 \text{ }^\circ\text{C}$ before all of the measurements. The pure water flux was calculated by eq 1

$$J = \frac{Q}{A \times t} \quad (1)$$

where J is the membrane flux ($\text{L}/\text{m}^2 \cdot \text{h} \cdot \text{bar}$), Q is the volume of permeated water (L), A is the membrane area (m^2), and t is the permeation time (h).

The rejection of the membrane was measured by the filtration of 0.3 g/L dextran (different molecular weights) solution. The dextran concentrations were measured by a total organic carbon analyzer (TNM-1, Shimadzu), and the rejection was calculated by eq 2

$$R = \frac{(C_f - C_p)}{C_f} \times 100\% \quad (2)$$

where R is the rejection ratio and C_f and C_p are the solute concentrations of feed and permeate solutions (mg/L), respectively. The mean effective pore size distribution was obtained based on the rejection data, according to the reported method.⁶¹

For the antifouling test, pure water was first passed through the membrane at least half an hour until the flux remained stable. After testing the pure water flux (J_{w1}), water was replaced by the BSA solutions. The flux was measured again for 3 h with the BSA solution, marked as J_p . Finally, the membrane was cleaned with pure water for 20 min by cross-flow, and the water flux was measured again, marked as J_{w2} . The FRR was calculated by the following expression

$$\begin{aligned} \text{FRR} &= \frac{J_{w2}}{J_{w1}} \times 100 \\ \text{Fr} &= \frac{J_{w1} - J_p}{J_{w1}} \times 100 \\ \text{Fir} &= \frac{J_{w1} - J_{w2}}{J_{w1}} \times 100 \end{aligned} \quad (3)$$

■ ASSOCIATED CONTENT

Supporting Information

The Supporting Information is available free of charge on the ACS Publications website at DOI: 10.1021/acsomega.7b02094.

Separation property, contact angle and mechanical properties of ETA-modified PAN by the static procedure at different temperatures, N_2 adsorption/desorption result, pore size distribution, experimental materials, and ETA modification mechanism (PDF)

■ AUTHOR INFORMATION

Corresponding Author

*E-mail: hyang@ecust.edu.cn.

ORCID

Hu Yang: 0000-0001-9411-2553

Zhenliang Xu: 0000-0002-1436-4927

Notes

The authors declare no competing financial interest.

■ ACKNOWLEDGMENTS

This work is supported by the National Natural Science Foundation of China (no. 21276075) for financial support.

■ REFERENCES

- Xie, M.; Shon, H. K.; Gray, S. R.; Elimelech, M. Membrane-based Processes for Wastewater Nutrient Recovery: Technology, Challenges, and Future Direction. *Water Res.* **2016**, *89*, 210–221.
- Gao, W.; Liang, H.; Ma, J.; Han, M.; Chen, Z.-l.; Han, Z.-s.; Li, G.-b. Membrane fouling control in ultrafiltration technology for drinking water production: A review. *Desalination* **2011**, *272*, 1–8.
- Zhang, R.; Liu, Y.; He, M.; Su, Y.; Zhao, X.; Elimelech, M.; Jiang, Z. Antifouling membranes for sustainable water purification: strategies and mechanisms. *Chem. Soc. Rev.* **2016**, *45*, 5888–5924.
- Rana, D.; Matsuura, T. Surface Modifications for Antifouling Membranes. *Chem. Rev.* **2010**, *110*, 2448–2471.

(5) Ayyavoo, J.; Nguyen, T. P. N.; Jun, B.-M.; Kim, I.-C.; Kwon, Y.-N. Protection of polymeric membranes with antifouling surfacing via surface modifications. *Colloids Surf., A* **2016**, *506*, 190–201.

(6) Li, Y.; He, G.; Wang, S.; Yu, S.; Pan, F.; Wu, H.; Jiang, Z. Recent advances in the fabrication of advanced composite membranes. *J. Mater. Chem. A* **2013**, *1*, 10058–10077.

(7) Zhang, P.-Y.; Xu, Z.-L.; Ma, X.-H.; Yang, H.; Wu, W.-Z.; Wei, Y.-M.; Liu, Y.-D. Fabrication and characterization of PVDF hollow fiber membranes employing in-situ self-assembly modulation concept. *J. Membr. Sci.* **2015**, *486*, 119–131.

(8) Yan, H.; Lu, X.; Wu, C.; Sun, X.; Tang, W. Fabrication of a super-hydrophobic polyvinylidene fluoride hollow fiber membrane using a particle coating process. *J. Membr. Sci.* **2017**, *533*, 130–140.

(9) Zhao, S.; Yao, Y.; Ba, C.; Zheng, W.; Economy, J.; Wang, P. Enhancing the performance of polyethylenimine modified nano-filtration membrane by coating a layer of sulfonated poly(ether ether ketone) for removing sulfamerazine. *J. Membr. Sci.* **2015**, *492*, 620–629.

(10) Arena, J. T.; McCloskey, B.; Freeman, B. D.; McCutcheon, J. R. Surface modification of thin film composite membrane support layers with polydopamine: Enabling use of reverse osmosis membranes in pressure retarded osmosis. *J. Membr. Sci.* **2011**, *375*, 55–62.

(11) Ulbricht, M.; Yang, H. Porous Polypropylene Membranes with Different Carboxyl Polymer Brush Layers for reversible Protein Binding via Surface-Initiated Graft Copolymerization. *Chem. Mater.* **2005**, *17*, 2622–2631.

(12) Bojko, A.; Andreatta, G.; Montagne, F.; Renaud, P.; Pugin, R. Fabrication of thermo-responsive nano-valve by grafting-to in melt of poly(N-isopropylacrylamide) onto nanoporous silicon nitride membranes. *J. Membr. Sci.* **2014**, *468*, 118–125.

(13) Luo, J.; Meyer, A. S.; Mateiu, R. V.; Kalyani, D.; Pinelo, M. Functionalization of a Membrane Sublayer Using Reverse Filtration of Enzymes and Dopamine Coating. *ACS Appl. Mater. Interfaces* **2014**, *6*, 22894–22904.

(14) Zhu, W.-P.; Gao, J.; Sun, S.-P.; Zhang, S.; Chung, T.-S. Poly(amidoamine) dendrimer (PAMAM) grafted on thin film composite (TFC) nanofiltration (NF) hollow fiber membranes for heavy metal removal. *J. Membr. Sci.* **2015**, *487*, 117–126.

(15) Weinman, S. T.; Husson, S. M. Influence of chemical coating combined with nanopatterning on alginate fouling during nanofiltration. *J. Membr. Sci.* **2016**, *513*, 146–154.

(16) Bernstein, R.; Antón, E.; Ulbricht, M. UV-Photo Graft Functionalization of Polyethersulfone Membrane with Strong Polyelectrolyte Hydrogel and Its Application for Nanofiltration. *ACS Appl. Mater. Interfaces* **2012**, *4*, 3438–3446.

(17) Yang, H.; Lazos, D.; Ulbricht, M. Thin, Highly Crosslinked Polymer Layer Synthesized via Photoinitiated Graft Copolymerization on a Self-Assembled-Monolayer-Coated Gold Surface. *J. Appl. Polym. Sci.* **2005**, *97*, 158–164.

(18) Cai, T.; Wang, R.; Yang, W. J.; Lu, S.; Neoha, K.-G.; Kang, E.-T. Multi-functionalization of poly(vinylidene fluoride) membranes via combined “grafting from” and “grafting to” approaches. *Soft Matter* **2011**, *7*, 11133–11143.

(19) Mauter, M. S.; Wang, Y.; Okemgbo, K. C.; Osuji, C. O.; Giannelis, E. P.; Elimelech, M. Antifouling Ultrafiltration Membranes via Post-Fabrication Grafting of Biocidal Nanomaterials. *ACS Appl. Mater. Interfaces* **2011**, *3*, 2861–2868.

(20) Yang, Q.; Ulbricht, M. Novel Membrane Adsorbers with Grafted Zwitterionic Polymers Synthesized by Surface-Initiated ATRP and Their Salt-Modulated Permeability and Protein Binding Properties. *Chem. Mater.* **2012**, *24*, 2943–2951.

(21) Ben-Sasson, M.; Zodrow, K. R.; Gengeng, Q.; Kang, Y.; Giannelis, E. P.; Elimelech, M. Surface Functionalization of Thin-Film Composite Membranes with Copper Nanoparticles for Antimicrobial Surface Properties. *Environ. Sci. Technol.* **2014**, *48*, 384–393.

(22) Dong, H.-B.; Xu, Y.-Y.; Yi, Z.; Shi, J.-L. Modification of polysulfone membranes via surface-initiated atom transfer radical polymerization. *Appl. Surf. Sci.* **2009**, *255*, 8860–8866.

- (23) Farjadian, F.; Schwark, S.; Ulbricht, M. Novel functionalization of porous polypropylene microfiltration membranes: via grafted poly(aminoethyl methacrylate) anchored Schiff bases toward membrane adsorbers for metal ions. *Polym. Chem.* **2015**, *6*, 1584–1593.
- (24) Lambla, M. Reactive Extrusion, A New Tool for the Diversification of Polymeric Materials. In *Rheological Fundamentals of Polymer Processing*; Covas, J. A., Agassant, J. F., Diogo, A. C., Vlachopoulos, J., Walters, K., Eds.; NATO ASI Series; Springer, 1995; Vol. 302, pp 437–454.
- (25) Yao, X.; Zhang, Y.; Du, L.; Liu, J.; Yao, J. Review of the applications of microreactors. *Renewable Sustainable Energy Rev.* **2015**, *47*, 519–539.
- (26) Hansen, S. H.; Helboe, P.; Thomsen, M. Dynamically-modified silica—an alternative to reversed-phase high-performance liquid chromatography on chemically bonded phases. *J. Pharm. Biomed. Anal.* **1984**, *2*, 165–172.
- (27) Sejoubsari, R. M.; Martinez, A. P.; Kutes, Y.; Wang, Z.; Dobrynin, A. V.; Adamson, D. H. Grafting-Through: Growing Polymer Brushes by Supplying Monomers through the Surface. *Macromolecules* **2016**, *49*, 2477–2483.
- (28) Shen, Y. J.; Wu, G. X.; Xu, S. G.; Zhong, H.; Zhang, S. L.; Zhang, X. Z.; Zhao, X. H.; WU, T.; Zhang, W. J. Gas-initiation under UV and liquid-grafting polymerization on the surface of polysulfone hollow fiber ultrafiltration membrane by dynamic method. *J. Environ. Sci.* **2005**, *17*, 465–468.
- (29) He, M.; Yao, J.; Li, L.; Zhong, Z.; Chen, F.; Wang, H. Aqueous solution synthesis of ZIF-8 films on a porous nylon substrate, by contra-diffusion method. *Microporous Mesoporous Mater.* **2013**, *179*, 10–16.
- (30) Seo, M.; Moll, D.; Silvis, C.; Hillmyer, M. A. Interfacial Polymerization of Reactive Block Polymers for the Preparation of Composite Ultrafiltration Membranes. *Ind. Eng. Chem. Res.* **2014**, *53*, 18575–18579.
- (31) Brown, A. J.; Brunelli, N. A.; Eum, K.; Rashidi, F.; Johnson, J. R.; Koros, W. J.; Jones, C. W.; Nair, S. Interfacial microfluidic processing of metal-organic framework hollow fiber membranes. *Science* **2014**, *345*, 72–75.
- (32) Van Goethem, C.; Verbeke, R.; Hermans, S.; Bernstein, R.; Vankelecom, I. F. J. Controlled positioning of MOFs in interfacially polymerized thin-film nanocomposites. *J. Mater. Chem. A* **2016**, *4*, 16368–16376.
- (33) Majeed, S.; Fierro, D.; Buhr, K.; Wind, J.; Du, B.; Boschetti-de-Fierro, A.; Abetz, V. Multi-walled carbon nanotubes (MWCNTs) mixed polyacrylonitrile (PAN) ultrafiltration membranes. *J. Membr. Sci.* **2012**, *403–404*, 101–109.
- (34) Zhao, R.; Wang, Y.; Li, X.; Sun, B.; Li, Y.; Ji, H.; Qiu, J.; Wang, C. Surface Activated Hydrothermal Carbon-Coated Electrospun PAN Fiber Membrane with Enhanced Adsorption Properties for Herbicide. *ACS Sustainable Chem. Eng.* **2016**, *4*, 2584–2592.
- (35) Zhang, B.; Wang, D.; Wu, Y.; Wang, Z.; Wang, T.; Qiu, J. Modification of the desalination property of PAN-based nanofiltration membranes by a preoxidation method. *Desalination* **2015**, *357*, 208–214.
- (36) Koushkbaghi, S.; Jafari, P.; Rabiei, J.; Irani, M.; Aliabadi, M. Fabrication of PET/PAN/GO/Fe₃O₄ nanofibrous membrane for the removal of Pb(II) and Cr(VI) ions. *Chem. Eng. J.* **2016**, *301*, 42–50.
- (37) Zhao, X.; Su, Y.; Chen, W.; Peng, J.; Jiang, Z. Grafting perfluoroalkyl groups onto polyacrylonitrile, membrane surface for improved fouling release property. *J. Membr. Sci.* **2012**, *415*, 824–834.
- (38) Meng, H.; Cheng, Q.; Li, C. Polyacrylonitrile-based zwitterionic ultrafiltration membrane. with improved anti-protein-fouling capacity. *Appl. Surf. Sci.* **2014**, *303*, 399–405.
- (39) Mei, S.; Xiao, C.; Hu, X.; Shu, W. Hydrolysis modification of PVC/PAN/SiO₂ composite hollow fiber membrane. *Desalination* **2011**, *280*, 378–383.
- (40) Abedi, M.; Sadeghi, M.; Chenar, M. P. Improving antifouling performance of PAN hollow fiber membrane using surface modification method. *J. Taiwan Inst. Chem. Eng.* **2015**, *55*, 42–48.
- (41) Liu, W.; Cai, M.; He, Y.; Wang, S.; Zheng, J.; Xu, X. Development of antibacterial polyacrylonitrile membrane modified with a covalently immobilized lysozyme. *RSC Adv.* **2015**, *5*, 84432–84438.
- (42) Tripathi, B. P.; Dubey, N. C.; Subair, R.; Choudhury, S.; Stamm, M. Enhanced hydrophilic and antifouling polyacrylonitrile membrane with polydopamine modified silica nanoparticles. *RSC Adv.* **2016**, *6*, 4448–4457.
- (43) Mahlici, F. Y.; Altinkaya, S. A.; Yurekli, Y. Preparation and characterization of polyacrylonitrile membranes modified with polyelectrolyte deposition for separating similar sized proteins. *J. Membr. Sci.* **2012**, *415–416*, 383–390.
- (44) Habibi, S.; Nematollahzadeh, A.; Mousavi, S. A. Nano-scale modification of polysulfone membrane matrix and the surface for the separation of chromium ions from water. *Chem. Eng. J.* **2015**, *267*, 306–316.
- (45) Lasseguette, E.; Rouch, J.-C.; Remigy, J.-C. Hollow-Fiber Coating: Application to Preparation of Composite Hollow-Fiber Membrane for Gas Separation. *Ind. Eng. Chem. Res.* **2013**, *52*, 13146–13158.
- (46) Chiang, W.-Y.; Hu, C.-M. Studies of reactions with polymers. VI. The modification of PAN with primary amines. *J. Polym. Sci., Part A: Polym. Chem.* **1990**, *28*, 1623–1636.
- (47) El-Newehy, M. H.; Alamri, A.; Al-Deyab, S. S. Optimization of amine-terminated polyacrylonitrile synthesis and characterization. *Arabian J. Chem.* **2014**, *7*, 235–241.
- (48) Wang, J.; Yue, Z.; Ince, J. S.; Economy, J. Preparation of nanofiltration membranes from polyacrylonitrile ultrafiltration membranes. *J. Membr. Sci.* **2006**, *286*, 333–341.
- (49) Xu, J.; Feng, X.; Chen, P.; Gao, C. Development of an antibacterial copper (II)-chelated polyacrylonitrile ultrafiltration membrane. *J. Membr. Sci.* **2012**, *413–414*, 62–69.
- (50) Parashuram, K.; Maurya, S. K.; Rana, H. H.; Singh, P. S.; Ray, P.; Reddy, A. V. R. Tailoring the molecular weight cut off values of polyacrylonitrile based hollow fibre ultrafiltration membranes with improved fouling resistance by chemical modification. *J. Membr. Sci.* **2013**, *425–426*, 251–261.
- (51) He, S.; Liu, W.; Ye, J.; Wang, S.; Xu, X. Grafting of oligodeoxynucleotide hairpin onto membrane surface to improve its anti-fouling performance. *Desalination* **2015**, *357*, 267–274.
- (52) Zhu, J.; Su, Y.; Zhao, X.; Li, Y.; Zhang, R.; Fan, X.; Ma, Y.; Liu, Y.; Jiang, Z. Constructing a zwitterionic ultrafiltration membrane surface via multisite anchorage for superior long-term antifouling properties. *RSC Adv.* **2015**, *5*, 40126–40134.
- (53) Hu, Y.; Lü, Z.; Wei, C.; Yu, S.; Liu, M.; Gao, C. Separation and antifouling properties of hydrolyzed PAN hybrid membranes prepared via in-situ sol-gel SiO₂nanoparticles growth. *J. Membr. Sci.* **2018**, *545*, 250–258.
- (54) Nazri, N. A. M.; Lau, W. J.; Ismail, A. F. Improving water permeability and anti-fouling property of polyacrylonitrile-based hollow fiber ultrafiltration membranes by surface modification with polyacrylonitrile-g-poly(vinyl alcohol) graft copolymer. *Korean J. Chem. Eng.* **2015**, *32*, 1853–1863.
- (55) Zhao, X.; He, C. Efficient Preparation of Super Antifouling PVDF Ultrafiltration Membrane with One Step Fabricated Zwitterionic Surface. *ACS Appl. Mater. Interfaces* **2015**, *7*, 17947–17953.
- (56) Lü, X.; Wang, X.; Guo, L.; Zhang, Q.; Guo, X.; Li, L. Preparation of PU modified PVDF antifouling membrane and its hydrophilic performance. *J. Membr. Sci.* **2016**, *520*, 933–940.
- (57) Mou, Y.; Yang, H.; Xu, Z. Morphology, Surface Layer Evolution, and Structure–Dye Adsorption Relationship of Porous Fe₃O₄ MNPs Prepared by Solvothermal/Gas Generation Process. *ACS Sustainable Chem. Eng.* **2017**, *5*, 2339–2349.
- (58) Pourjafar, S.; Rahimpour, A.; Jahanshahi, M. Synthesis and characterization of PVA/PES thin film composite nanofiltration membrane modified with TiO₂ nanoparticles for better performance and surface property. *J. Ind. Eng. Chem.* **2012**, *18*, 1398–1405.

(59) Boributh, S.; Chanachai, A.; Jiratananon, R. Modification of PVDF membrane by chitosan solution for reducing protein fouling. *J. Membr. Sci.* **2009**, *342*, 97–104.

(60) Bi, Q.; Li, Q.; Tian, Y.; Lin, Y.; Wang, X. Hydrophilic modification of poly(vinylidene fluoride) membrane with poly(vinyl pyrrolidone) via a cross-linking reaction. *J. Appl. Polym. Sci.* **2013**, *127*, 394–401.

(61) Yang, Q.; Chung, T.-S.; Santoso, Y. E. Tailoring pore size and pore size distribution of kidney dialysis hollow fiber membranes via dual-bath coagulation approach. *J. Membr. Sci.* **2007**, *290*, 153–163.